Physiological and Molecular Plant Pathology 144 (2026) 103244

Contents lists available at ScienceDirect

Physiological and Molecular Plant Pathology

journal homepage: www.elsevier.com/locate/pmpp

Pinolidoxin production by *Ascochyta pinodes* during pea infection: Insights from *in planta* metabolomics

Pierluigi Reveglia [a], Sara Rodriguez-Mena [b], José E. Yuste [c], Lucia Lecce [a], Diego Rubiales [b], Eleonora Barilli [b,*]

[a] Department of Clinical and Experimental Medicine, University of Foggia, Foggia, 71122, Italy
[b] Institute for Sustainable Agriculture, CSIC, Córdoba, 14004, Spain
[c] Metabolomics Platform, Centro de Edafología y Biología Aplicada del Segura, CSIC, Murcia, 30100, Spain

ARTICLE INFO

Keywords:
Ascochyta blight
Pisum sativum
Non-targeted metabolomics
Targeted metabolomics
Pinolidoxin

ABSTRACT

Ascochyta pinodes, the leading cause of Ascochyta blight in pea, poses a significant threat to crop yield and quality; nevertheless, limited investigations have utilized metabolomics to study the *Pisum sativum-A. pinodes* pathosystem. This study presents the first *in planta* metabolomics-based study focused on the detection of phytotoxic metabolites produced by *A. pinodes*. Among the fungal metabolites screened, only pinolidoxin was detected in infected tissues, peaking at 48 h post-inoculation. This temporal association suggests a possible effector-like role for pinolidoxin in promoting early infection through interference with host signaling pathways. Furthermore, non-targeted metabolomics-based analysis of *A. pinodes* infection in susceptible and resistant pea cultivars, Messire and Radley, was also carried out, revealing cultivar-specific metabolic responses in the susceptible cultivar. Messire showed strong activation of phenylpropanoid metabolism, especially flavonoids and hydroxycinnamic acids, while the resistant cv. Radley upregulated amino acids and derivatives, suggesting differences in the defense strategy based on adjustments to primary metabolism, which could be related to Radley resistance. This work highlights the complexity of host-pathogen interactions. It underscores the importance of multi-omics approaches in identifying molecular targets for gaining deeper systems-level insight into pea defense strategies, thereby supporting the development of improved disease-resistant legume varieties.

1. Introduction

Pea (*Pisum sativum* L.) is a cool-season annual legume crop widely cultivated for human and animal consumption, as well as forage. Its ability to fix atmospheric nitrogen, along with its high-quality protein and amino acid content, makes it a key crop for sustainable agriculture [1]. However, its production is mainly limited by root and aerial diseases, with Ascochyta blight being one of the most significant foliar diseases [2]. Ascochyta blight, also known as “black spot” disease, is widely distributed across Europe, Canada, Australia, USA and China. It causes dark-brown necrotic lesions on the aboveground parts of the plants, negatively affecting pods and seed quality and quantity [3]. This disease is caused by a complex of fungal species including, *Ascochyta pisi, A. pinodes*, *Phoma medicaginis* var. *pinodella*, *P. koolunga* and *P. glomerata*, which could co-infect or produce the disease individually [4]. Among these, *A. pinodes* (teleomorph *Peyronellaea pinodes*, syn. *Mycospharella pinodes* and *Didymella pinodes*) is the most widespread and damaging species [2].

Regarding plant defense, resistance to Ascochyta blight in pea has been associated with the plant's ability to reduce pathogen colony establishment and lesion size. This is achieved through the induction of several defense mechanisms including pisatin accumulation, protein cross-linking, hydrogen peroxide accumulation and localized death of epidermal cells [5,6]. On the other hand, as other fungal pathogens, Ascochyta blight fungi are known to produce a range of phytotoxic metabolites that could act as virulence factors contributing to fungal pathogenicity and the development of disease symptoms in plants [7,8]. These metabolites belong to different classes, including macrolides, polyketides, anthraquinones, meroterpenoids, solanapyrones and peptides.

Previous studies on the specialized metabolites produced by *A. pinodes* have already been performed due to the importance and virulence of the pathogen in pea [2]. Early research by Evidente and co-authors [9], demonstrated that fungal isolates cultured on sterilized wheat

* Corresponding author
E-mail address: ebarilli@ias.csic.es (E. Barilli).

https://doi.org/10.1016/j.pmpp.2026.103244
Received 7 November 2025; Received in revised form 24 April 2026; Accepted 27 April 2026
Available online 4 May 2026
0885-5765/© 2026 The Authors. Published by Elsevier Ltd. This is an open access article under the CC BY license (http://creativecommons.org/licenses/by/4.0/).

produced a major phytotoxin, named pinolidoxin, which was identified as a novel macrocyclic lactone with potent phytotoxicity towards peas and other plants. More recent studies identified additional metabolites from an aggressive Spanish isolate, including pinolide, a newly characterized nonenolide, and three others related nonenolides: pinolidoxin, herbarumin II, and 2-epi-herbarumin II [10].

Nevertheless, similar to many fungal phytotoxins reported in the literature, these compounds have been characterized only *in vitro* culture-based studies. This limitation is prevalent in fungal phytotoxin research, where ecological relevance is frequently assumed rather than empirically demonstrated. Recent advances in non-targeted and targeted metabolomics have facilitated high-throughput *in vitro* screening and enabled chemotaxonomic studies by identifying metabolites produced and utilized during the fungal life cycle, as demonstrated in *Ascochyta* spp. [11]. Furthermore, these techniques now allow for the direct detection of pathogen-derived metabolites in infected host tissues, offering new insights into their functional roles during infection under natural conditions [12–15]. Indeed, metabolomics approaches have successfully detected a few fungal phytotoxins *in planta*, including guignardic acid [12] and (R)-mellein [15]. However, the production of pinolidoxin during host colonization remains unconfirmed. This knowledge gap is significant because pinolidoxin's role in disease development, although extensively characterized *in vitro*, has not been validated under natural infection conditions. Addressing this gap is essential for elucidating the chemical mechanisms underlying host-pathogen interactions in the *P. sativum-A. pinodes* pathosystem and for advancing understanding of how fungal metabolites contribute to pathogenesis in their natural context.

Few studies have applied metabolomics to investigate the *P. sativum-A. pinodes* pathosystem. Most multi-omics research to date has focused on the host role in the interaction, with particular emphasis on beneficial microbial symbionts such as rhizobia and mycorrhizae. Integrative proteomic and metabolomic analyses demonstrate that these symbiotic relationships can induce systemic resistance in pea plants by modulating RNA metabolism, protein synthesis, redox balance, and hormonal signaling pathways, as well as by increasing the accumulation of defence-related secondary metabolites [16]. Additionally, rhizobial inoculation correlates with reduced disease severity and enhanced seed quality through metabolomic and proteomic changes involving redox regulation, cell wall modifications, and stress-related proteins [17]. More recently, targeted proteomics has been used to identify host-derived resistance markers associated with quantitative disease tolerance, facilitating the characterization of defence-related peptides and pathways linked to resistance against *A. pinodes* [18].

These studies have significantly advanced the understanding of plant-mediated resistance mechanisms and host molecular responses to infection, although they have primarily adopted a plant-centered perspective. This fact, together with previous research on *A. pinodes* that focused solely on *in vitro* analyses of the pathogen's phytotoxins [9,10], has left the production and accumulation of fungal specialized metabolites during host colonization largely unexplored in this pathosystem. This knowledge gap is critical, as *in vitro* studies do not fully replicate the metabolic conditions present during infection, and plant-centered omics approaches do not directly reveal pathogen-derived metabolite dynamics. The present investigation, which seeks to explore the *in planta* detection of pinolidoxin and provides direct evidence of fungal metabolite accumulation during host colonization, could help move beyond previous *in vitro* observations and offer new insight into the chemical basis of *A. pinodes* pathogenicity.

Building on this context, firstly, the virulence of five *A. pinodes* isolates of different origins and aggressiveness was evaluated by inoculating two pea cultivars with different levels of resistance: cv. Messire (susceptible) and cv. Radley (partially resistant). Then, the production of specific metabolites, including pinolidoxin, produced *in vitro* by the isolates was investigated. Based on the results of these two assays, the isolate with the highest production of pinolidoxin and the highest virulence was selected for non-targeted metabolomic profiling, followed by inoculation and *in planta* metabolic response characterization in both cultivars at different time points.

To our knowledge, this is the first report of *in planta* detection and quantification of this metabolite in the *A. pinodes*-pea interaction. This work also represents the first use of joint untargeted and targeted metabolomics in this system to study the temporal dynamics of fungal specialized metabolites during host colonization. Unlike previous *in vitro* observations, this approach provides new insights into this plant-pathogen relationship.

2. Materials and methods

2.1. General experimental procedures

Solvents EtOAc and $CHCl_3$ were purchased from Panreac AppliChem (Barcelona, Spain), while acetonitrile (ACN), Na_2SO_4 and 0.22 μm syringe filter were purchased from Merck (Darmstadt, Germany). Ascosalipyrone and ascosalytoxin were isolated from *in vitro* cultures of *Ascochyta fabae* [19], while pinolidoxin was isolated from *A. pinodes* [10]. The identity and purity of all standard metabolites were checked by Nuclear Magnetic Resonance (NMR) analysis, and the synthesis of diacetyl-pinolidoxin was carried out at the University of Naples, Federico II. As Internal Standards (IS) for the UHPLC-QTOF-HRMS analysis, lidocaine analytical standard and 2-hydroxy-1,4-naphthoquinone for UHPLC-QTRAP, purchased from Sigma-Aldrich (St. Louis, Missouri, USA), were used. The LC-MS/MS platform for targeted analysis consisted of a UHPLC (Nexera Series LC-40, Shimadzu, Kyoto, Japan) coupled to a hybrid triple quadrupole/-linear ion trap tandem mass spectrometer (QTRAP 4500, AB Sciex, Framingham, MA, USA). The LC-MS/MS platform for non-targeted metabolomics consisted of UHPLC Acquity UPLC- I-class system (Waters Corporations, Milford, MA, USA), MaXis Impact QTOF mass spectrometer (Bruker Daltonics, Bremen, Germany).

2.2. Fungal isolates

Five *A. pinodes* isolates (CO99, FR88, PO03, JAP03 and ANN13), with different origins and aggressiveness on pea, were used (Supplementary Table 1) [20,21]. All of them belong to the Institute for Sustainable Agriculture (IAS-CSIC) fungal collection. They were monoconidial and preserved on sterile cellulose filter papers. Prior to use, isolates were multiplied on Petri dishes with potato dextrose agar (PDA) medium (60 mL/L PDA + 60 mg/L chloramphenicol + 50 mg/L ampicillin) at 23 ± 2 °C subjected to 16 h light/8 h dark photoperiod for 13 days.

2.3. Cultural conditions for Ascochyta pinodes isolates

Each isolate was grown in Erlenmeyer flask containing 200 mL of modified Czapek−Dox medium (5% glucose, 0.1% yeast extract,0.05% K_2HPO_4, 0.2% $NaNO_3$, 0.05% $MgSO_4{\cdot}7H_2O$, and 0.001%$FeSO_4{\cdot}7H_2O$). Three biological replicates for each isolate were grown. Each flask was inoculated with 10 mycelial plugs (of 5 mm^2 each) of a 10-days-old mycelial plate of each isolate on PDA. This liquid culture was incubated for 21 days at 20 °C in darkness on an orbital shaker set at 150 rpm. Then the contents of the flasks were centrifuged at 8000g, the mycelium discarded and the supernatant cultured filtrate stored at −20 °C before extraction.

2.4. Extraction of specialized metabolites from A. pinodes in vitro culture

The culture filtrates (200 mL) of modified Czapek−Dox medium obtained from the five *A. pinodes* isolates were exhaustively extracted with EtOAc (3 x 300 mL) using a separatory funnel. The organic extracts of each isolate were combined, dried (Na_2SO_4), and evaporated under reduced pressure yielding dark-brown solid residues.

2.5. Plant material

Two pea cultivars with different levels of resistance to *A. pinodes* were used, as cv. Radley (partially resistant) and cv. Messire (susceptible) [20,22]. Seeds were scarified and pre-germinated in Petri dishes with wet paper in darkness at 23 ± 2 °C. Germinated seeds were sown in 200 mL plastic pots (6 x 6 × 10 cm) with peat. Pots were placed in plastic trays (8 x 6 pots per tray) and located under controlled conditions in growing chambers at the IAS-CSIC with 24 ± 2 °C, 65% relative humidity (RH), 12:12 h day:night photoperiod with 150 μmol m^{-2} s^{-1}, until 4th leaf was completely expanded (around 10 days after sowing).

2.6. Plant inoculation and sampling

For plants inoculation, a conidiospore suspension was prepared by flooding PDA culture plates with autoclaved distilled water and scraping the colony surface with a scalpel. The resulting suspension was filtered with a sterile cheesecloth and spore concentration determined using a Ross-Fushental hemocytometer. Spore concentration was adjusted to 500,000 spores/mL and Tween-20 (20 μL/100 mL) added as wetting agent [21]. For pathogenicity assays, the experiment followed a completely randomized design including three independent biological replicates per fungal isolate and pea genotype. Each biological replicate consisted of five pots per treatment, with two plants per pot (*i.e.*, 10 plants per replicate). Plants per treatment were inoculated by manually spraying 1 mL of the spore suspension per plant. Five pots with 2 plants each of the uninoculated pea cv. Messire and Radley were also included in each replication as a check. Plants were incubated for 24 h at 20 °C in complete darkness and 100% relative humidity, then returned to a bench in the growth chamber, with conditions described above. Ten days after the inoculation, the diseases symptoms were visually assessed following the 0 to 5 disease rate scale described by Roger and Tivoli [23] where 0 = completely healthy plant, 1 = few scattered flecks, 2 = numerous flecks, 3 = 15% of the foliar part with necrosis and appearance of coalescent necrosis, 4 = 50% of the foliar part with necrosis or dehydrated, 5 = 100% of the foliar part dehydrated. The metabolomic *in planta* assay was performed with the most virulent *A. pinodes* isolate, by using the same methodology and experimental design as for the pathogenic assay. Leaf samples were collected at 24, 48 and 96 h after inoculation (hai). The metabolomic experiment followed a factorial design including two pea genotypes (Messire and Radley), two treatments (inoculated and uninoculated), and three sampling time points. For each combination of genotype × treatment × time point, four independent biological replicates were collected. Each biological replicate consisted of pooled material from two fully expanded leaves at the 4-5 leaf stage, sampled from different plants within the same treatment group to account for plant-to-plant variability. In total, this resulted in four biological replicates per experimental condition at each time point. Samples were placed in labelled paper envelopes and immediately weighed, frozen in liquid nitrogen and stored at −20 °C until use.

2.7. Extraction of metabolites from pea plants

For metabolomics analysis, the frozen tissue was homogenized in liquid nitrogen into a fine powder using a pestle and mortar. Subsequently, 300 mg of the homogenized powder was transferred into pre-cooled 15 mL glass centrifuge tubes and then 3 mL of MeOH, 1.2 mL of $CHCl_3$ and 0.6 mL of water (2.5: 1: 0.5, vol/vol) were added to each vial. After a mixed step by vortexing for 30 s, glass tubes were agitated for 30 min at 4 °C. To improve the collection of all three components, 3 mL of $CHCl_3$ and 1.5 mL of water (2:1 vol/vol) were added to the vials. For phase separation, extracts were centrifuged at 3000 rpm for 10 min at 4 °C. First, the upper (high polar and middle polar metabolites) phase was collected and transferred to plastic 5 mL Eppendorf tubes. The bottom (lipids and low polar metabolites) phase was removed and transferred to glass tubes. Lidocaine was spiked to each sample solution at a final 10 nmol/mL concentration. Equal volumes of each extract were combined to create three pooled quality control (QC) samples. The pooled QCs and the lidocaine area values were utilized to monitor the quality and robustness of the metabolomic analysis. All the extracts were filtered through a 0.22 μm syringe filter before LC-MS/MS analysis.

2.8. UHPLC-QTRAP apparatus and conditions

The LC-MS/MS platform consisted of a UHPLC (Nexera Series LC-40, Shimadzu, Kyoto, Japan) coupled to a hybrid triple quadrupole/linear ion trap tandem mass spectrometer (QTRAP 4500, AB Sciex, Framingham, MA, USA) equipped with a Turbo V ion source. Instrument control, data acquisition, and processing were performed using the associated Analyst 1.6 software. The LC separation was carried out on a C18 column Cortecs (4.6 mm × 50 mm, particle size 2.7 mm) from Waters (Milford, MA, USA). Elution was performed at a flow rate of 0.7 mL/min with water containing 0.1% (v/v) formic acid as eluent A and ACN (Merck, Darmstadt, Germany) containing 0.1% (v/v) formic acid as eluent B, employing a linear gradient from 95% to 5% A in 10 min, and holding the solvent concentration for 2 min. The injection duty cycle was 16 min, considering the column equilibration time. Q1 resolution was adjusted to 0.7 -0.1 amu fwhm for MRM, referred to as the unit resolution. Q3 was also set to the unit resolution in MRM mode. Mass Spectrometry analysis was carried out in positive ionization mode using an ion spray voltage of 5500 V. The nebulizer and the curtain gas flows were set at 35 psi using nitrogen. The Turbo V ion source was operated at 500 °C with the Gas 1 and 2 flow (nitrogen) set at 50 psi. Two suitable MRM transitions were selected for the metabolites: ascosalipyrone, ascosalytoxin and pinolidoxin, while one was selected for the ISs: 2-hydroxy-1,4-naphthoquinone and diacetyl-pinolidoxin. The compound-dependent parameters were optimized using the manual optimization protocol in tuning mode. The Declustering Potential (DP) was set to 45, the Exit Potential (EP) was set to 9, while the Q1 mass, the Q3 transition, and the best parameters are reported in Table 1. Chromatograms and structures of metabolites are reported in Supplementary Fig. 1. For sample analysis, two technical replicates were performed for each biological replicate.

2.9. UHPLC-QTRAP method validation

The method was validated by analyzing calibration curves, the limit of detection (LOD), the limit of quantification (LOQ), and within-day and between-day imprecision and inaccuracy. Calibration curves were obtained reporting the area ratio (metabolite area/IS area) against the injected mg of metabolites. Ten microliters of each standard solution were injected in triplicate to build the calibration curves. Three different curves were built for ascosalipyrone, ascosalytoxin, and pinolidoxin, respectively. LOD and LOQ were calculated as a magnitude of 3 and 10 times the standard deviation of the blank to the lower point of the

Table 1
Optimized Q1 mass, transitions and parameters for MRM experiment.

Metabolite	Precursor ion (*m/z*)	Product ion (*m/z*)	CE[a]	CXP[b]	RT[c] (min)
Ascosalipyrone	239.2 $[M+H]^+$	155.0 85.0	18	10	5.98
Ascosalytoxin	265.1 $[M+H]^+$	246.9 237.0	14	20	8.22
Pinolidoxin	338.7 $[M+H]^+$	209.0 181.1	11	14	7.65
Diacetyl-pinolidoxin	445.0 $[M+H]^+$	385.0	25	18	9.83
2-Hydroxy-1,4-Naphthoquinone	175.4 $[M+H]^+$	147.0	23	15	5.20

[a] Collision Energy.
[b] Collision Exit Potential.
[c] Retention Time.

standard level (Supplementary Table 2). Two quality control samples (QC) at two different concentration levels were used to assess the within-day and between-day variation. The within-day and between-day precision (RSD%) and accuracy (%), the former assessed by analyzing each level of QC samples five times in the same analytical run, and the latter assessed by analyzing each level of QC samples daily for five days, are reported in Supplementary Table 3. Precision and accuracy were automatically calculated by Multiquant software (version 2.0.2, AB SCIEX™, Ontario, Canada).

2.10. UHPLC-QTOF-HRMS apparatus and conditions

The UHPLC- QTOF-HRMS analysis was carried out by the Metabolomics Platform of the Centro de Edafología y Biología Aplicada del Segura (CEBAS-CSIC, Spain). Prior to mass spectrometric sample analysis, the chromatographic separation was realized using Acquity UHPLC- I-class system (Waters Corporations, Milford, MA, USA). Seven μL of the organic extract solution, were injected using a Sample Manager Fixed-Loop (SM-FL) (Waters Corporations, Milford, MA, USA). Chromatographic separation was performed on Poroshell 120 EC-C18 Agilent column (100 × 3 mm, 2.7 μm (Agilent Technologies, Waldbronn, Germany) operating at 30 °C and a flow rate of 0.4 mL/min in an Acquity I-Class column oven system (Waters Corporations, Milford, MA, USA). Compounds were separated using the following gradient conditions using H_2O + 0.1% formic acid (A) and ACN + 0.1% formic acid (B): 0–10 min, 1–18% phase-B; 10–16 min, 18–38% phase-B; 16–22 min, 38–95% phase-B. Finally, the phase B content was returned to the initial conditions (1%) for 1 min and the column re-equilibrated for five more min. Software Compass HyStar (version 3.2 Bruker Daltonics, Bremen, Germany) was used for the operation of the UHPLC systems. For sample analysis, two technical replicates were performed for each biological replicate. Two classes of quality control (QCs) were used for metabolomic analysis quality. QCs were MS grade MeOH/H2O +0.1% formic acid (70:30) blank and ± Lidocaine solution (10 nmol/mL) and were injected three times during the batch: beginning, middle and end. MaXis Impact QTOF mass spectrometer (Bruker Daltonics, Bremen, Germany) was utilized for QTOF-HRMS experiments in the organics extract of pea. For the DDA experiment, the mass spectrometer (QToF-MS) was operated in Auto MS/MS mode (ESI+). The ionization source capillary voltage was set to 4.5 kV in positive scanning mode. The nebulizer gas pressure was set to 2.0 bar. The dry gas temperature was set to 220 °C. Collision energy was stepping from 15 eV to 45 eV. The mass detection range was 50 to 1200 Da in positive ionization mode (+MS). The charge state was +1. The absolute threshold was 400 cts. The cycle time was 3 s with the spectra rate of 8 Hz. In DDA mode, the instrument spends 20% cycle time (0.6 s) on MS1 scanning and 80% cycle time (2.4 s) on MS^2 scanning. During MS/MS scanning period, if the precursor ion has a MS signal intensity larger than 1×10^5, MS^2 spectra rate is 4 Hz. For the experiments in DIA mode the mass spectrometer was operated in bbCID (broadband Collision Induced Dissociation) mode (ESI+), which is equivalent to DIA AIF or MS^{All} mode. Spectral acquisition was performed at alternating collision energies of 24 and 36 eV. Sodium formate cluster ions were applied for instrument mass calibration and for recalibration of individual raw data files. The Software's Compass Control and DataAnalysis (software versions 3.4 and 4.2, Bruker Daltonics, Bremen, Germany) were used for the operation of the mass spectrometer and for data acquisition.

2.11. Metabolite annotation and identification in A. pinodes extracts

The identification and quantification of ascosalipyrone, ascosalytoxin and pinolidoxin, was performed as described in the previous section. The raw LC-HRMS data from extracts of different *A. pinodes* isolates were converted into mzML format using MSConvert software (ProteoWizard, Palo Alto, CA, USA). Pre-processing of the data was carried out with MS-DIAL [24] using the following parameters: MS1 tolerance: 0.01 Da, MS2 tolerance: 0.05 Da, minimum peak height: 1000 (amplitude), alignment: A QC sample was used as the reference file with a retention time tolerance of 0.05 min. The processed metabolite ions were translated into structural information through MS-DIAL/MS-FINDER, integrated with MS/MS public databases. The databases used for peak identification included ESI(+)-MS/MS from authentic standards, ESI (+)-MS/MS from standards + bio+ *in silico*, MSMS-MassBankEU, MSMS-GNPS, MSMS-MassBank, MS/MS-Vaniya-Fiehn Natural Products Library. A thorough manual curation of all assigned peaks was conducted to ensure accuracy. Fungal metabolites were annotated based on confidence levels (A–C) [25,26] as detailed in Supplementary Table 4.

2.12. Metabolite annotation and identification in pea extracts

To fully exploit the differences in the metabolite profile obtained three chemoinformatic tools were integrated: MS-DIAL (Version 5.10) and MS-FINDER (Version 3.5) [24], MetaboAnalyst 6.0 [27]. The analysis of the non-targeted spectra obtained from pea extracts was conducted in the following steps: (i) the mzML files were pre-processed with MS-DIAL. The MS-DIAL parameters were MS1 tolerance of 0.01 Da; MS2 tolerance of 0.05 Da; minimum peak height of 1000 (amplitude); for alignment, a QC sample was used as reference file, and the retention time tolerance was set at 0.05 min. The metabolite ions were converted into structural information with MS-DIAL/MS-FINDER linked to MS/MS databases. The databases used for peak identification included ESI (+)-MS/MS from authentic standards, ESI(+)-MS/MS from standards + bio+*in silico*, MSMS-MassBankEU, MSMS-GNPS, MSMS-MassBank, MS/MS-Vaniya-Fiehn Natural Products Library. Prior to statistical analysis features with a blank contribution greater than 5% and those with a relative standard deviation (RSD) in Quality Control (QC) samples higher than 20% were removed. The tables included 269 features for $CHCl_3$ extracts and 389 for MeOH extracts; (ii) Univariate and multivariate statistical analyses were performed using MetaboAnalyst 6.0. Prior to statistical analysis, features with more than 50% missing values across the samples were excluded. Missing values were estimated using the sample-wise k-nearest neighbours (KNN) algorithm. Given that both positive and negative feature tables contained between 200 and 500 features, 10% of features with near-constant values were identified using the interquartile range (IQR), while features with small values were detected through mean value analysis and subsequently filtered out. Data were normalised by median, and specific transformation and scaling conditions for the datasets are reported in Supplementary Table 5. The datasets inoculated *vs* control and pea cv. Messire *vs* pea cv. Radley were analysed with PLS-DA to sharpen groups' separation and reveal the global profile changes and potential application for biomarker discovery according to metabolite composition. The VIP score cutoff value was 1.2 [28]. Cross-validation was carried out by 5-fold CV; Accuracy, R2 and Q2 values are reported in Supplementary Table 5. PCA was used to explore variation among the selected sampling times. Heatmaps showing clustering of the features were used to visualize the differences between samples using the top 20 (ANOVA p corrected for FDR <0.05) most significant features. For PCA and Heatmap visualization R software 4.2.3 packages ggplot2 and pheatmap were used [29,30]. Potential differences in the datasets were further investigated using Volcano plot with p-value corrected for FDR <0.05 and Fold Change (FC) > 5 as thresholds; (iii) the identification of significant features highlighted was carried out using MS-DIAL the score cutoff value was selected as 8. Significant metabolites with monoisotopic mass error within ±5 mDa with no proper match in the selected databases were manually screened for mass spectral peak matching and *in silico* fragmentation using MS-FINDER. Careful manual curation of all assigned peaks was carried out, and the metabolites were annotated according to confidence levels A-D [25,26], as described in Supplementary Table 6.

3. Results and discussion

3.1. Pathogenicity assay of A. pinodes isolates

As previously reported [20,22], cv. Radley exhibited resistance to all the tested isolates, while cv. Messire was susceptible. Among the tested isolates, CO99, FR88, and JAP03 induced the most pronounced symptoms on cv. Messire (Disease Score, DS = 5), suggesting a higher level of aggressiveness compared to PO33 and ANN13 (DS = 4). Additionally, some symptoms were also observed on cv. Radley with CO99 and FR88 isolates (DS = 2 and DS = 3, respectively). The observed symptoms are shown in Supplementary Fig. 2, which includes pictures of infected plants.

3.2. Quantification of known metabolites from the in vitro culture of selected A. pinodes isolate

A. pinodes is known to produce phytotoxic specialized metabolites [10]. As a starting point for investigating potential differences in the production of bioactive specialized metabolites among the five selected *A. pinodes* isolates, a targeted dereplication approach was employed. Three metabolites previously reported in other *Ascochyta* species were selected: ascosalipyrone and ascosalitoxin, available in-house because they were previously isolated from *A. fabae* [19], and pinolidoxin, a well-characterized phytotoxin from *A. pinodes* [10], kindly provided by collaborators at the University of Naples (Italy). Quantitative analysis was performed using a Quadrupole Ion Trap (QTRAP) mass spectrometry. Details of the analytical procedure are provided in the experimental section, and the results are summarised in Table 1. The amounts of targeted metabolites produced by selected *A. pinodes* isolates are reported in Table 2.

Notably, ascosalitoxin was not detected in any of the tested extracts. Ascosalipyrone was detected at trace levels, below the limit of quantification, in only two of the studied *A. pinodes* isolates, ANN13 and JAP03. Ascosalipyrone, a polyketide first isolated from *A. salicorniae*, is known for its antiplasmodial and antimicrobial activities, as well as for inhibiting tyrosine kinase p56lck and protein phosphatases [31,32]. In contrast, pinolidoxin was consistently detected in all isolates, though the quantities varied significantly. Importantly, *A. pinodes* FR88, the isolate exhibiting the highest pathogenicity in our pathogenicity assays, also produced the highest levels of pinolidoxin (0.048 ± 0.002 mg/g). Initially isolated in 1993 [9], pinolidoxin has been extensively studied for its potent phytotoxicity, also attracting interest in its total synthesis [33–35]. This metabolite was tested across a range of legumes and weed species, causing necrotic lesions regardless of host specificity [10]. These findings underscore its potential role as a virulence factor. Given the highest pathogenicity in our experimental condition and the elevated amounts of pinolidoxin detected in *A. pinodes* FR88, this isolate was selected for further investigation. Specifically, non-targeted metabolomic profiling was initiated to explore the full spectrum of specialized metabolites produced *in vitro*, followed by an analysis of metabolite production *in planta* during infection, with parallel monitoring of metabolic responses in pea cultivars at distinct infection stages, as described in the following sections.

3.3. Optimization of non-targeted metabolomics analysis and dereplication of specialized metabolites from A. pinodes isolate FR88

To further investigate specialized metabolite production, the extract of *A. pinodes* FR88 was examined using non-targeted metabolomics with an Ultra high-resolution liquid chromatography- Quadrupole time of fly (UHPLC-QTOF) system. This technique is a widely used analytical platform for non-targeted metabolomics due to its high throughput, sensitivity, and specificity. The common mass spectrometry (MS) data acquisition modes for recording metabolic signals are full-scan, data-dependent acquisition (DDA), and data-independent acquisition (DIA) [36]. In DDA mode, the MS instrument first performs a full-scan analysis, followed by MS^2 analysis on a list of precursor ions selected from the full-scan spectrum [37]. This allows for the acquisition of both quantitative information (from the full-scan) and structural information (from the MS^2 spectra) within the same sample analysis, facilitating simultaneous data processing and metabolite identification. The recent implementation of DIA in metabolomic studies has the potential to generate MS^2 spectra for all precursor ions. This capability enables the detection and identification of more metabolites, even at lower concentrations [38,39]. In DIA mode, the MS instrument cycles through the precursor ion *m/z* range with a large precursor ion mass width to simultaneously fragment multiple precursor ions. Commonly used DIA methods include all-ion fragmentation (AIF) (e.g., MSAll. MSE, bbCID) [40–42], where all precursors are fragmented, and sequential window acquisition of all theoretical fragment-ion spectra.

In this study, the organic extract of *A. pinodes* isolate FR88 was investigated using both DDA and DIA to determine the most suitable method for the experiment. Findings indicated that the DIA acquisition mode demonstrated the highest sensitivity. As illustrated in Fig. 1, which displays the base peak chromatogram (BPC) and intensities (cps) of the FR88 organic extract analysed in both DDA (AutoMS/MS, Fig. 1A) and DIA (bbCID_+MS, Fig. 1B), the intensity of the pinolide peak is significantly higher (a factor of five) in DIA mode compared to DDA mode.

This outcome is not surprising, given that previous comparisons have shown that DIA offers improved quantitative precision and MS^2 spectral coverage compared to DDA [36]. Considering that the experiment's goal is to investigate the production of specialized metabolites in plant tissue extracts, typically complex matrices with low metabolite quantities (ng/g of plant tissue), the DIA acquisition mode was selected for the non-targeted metabolomics analysis of pea extracts.

After selecting the DIA mode, the spectral data were analysed to identify specialized metabolites that had not been quantified through the targeted approach. This analysis allowed us to expand the range of potential fungal-detectable metabolites after inoculation. Chemoinformatic tools as MS-DIAL and MS-FINDER were used for spectral analysis, focusing on fungal metabolites documented in curated online databases. A complete list of the putatively identified metabolites can be found in Supplementary Table 4. In addition to the previously quantified compounds, five additional metabolites were putatively identified:

Table 2
Amount (mg/g of extract) of targeted metabolites produced by selected *A. pinodes* isolates.

Metabolite	*A. pinodes* isolate				
	ANN13 (mg/g)	CO99 (mg/g)	FR88 (mg/g)	JAP03 (mg/g)	PO03 (mg/g)
Ascosalipyrone	[a]<LOQ	[b] < LOD	<LOD	<LOQ	<LOD
Ascosalytoxin	[c]n.d.	n.d.	n.d.	n.d.	n.d.
Pinolidoxin	[d]0.003 ± 0.0002	0.005 ± 0.0002	0.048 ± 0.002	<LOD	0.026 ± 0.002

[a] Limit of Quantification.
[b] Limit of Detection.
[c] n.d.: not detected.
[d] Mean ± SD.

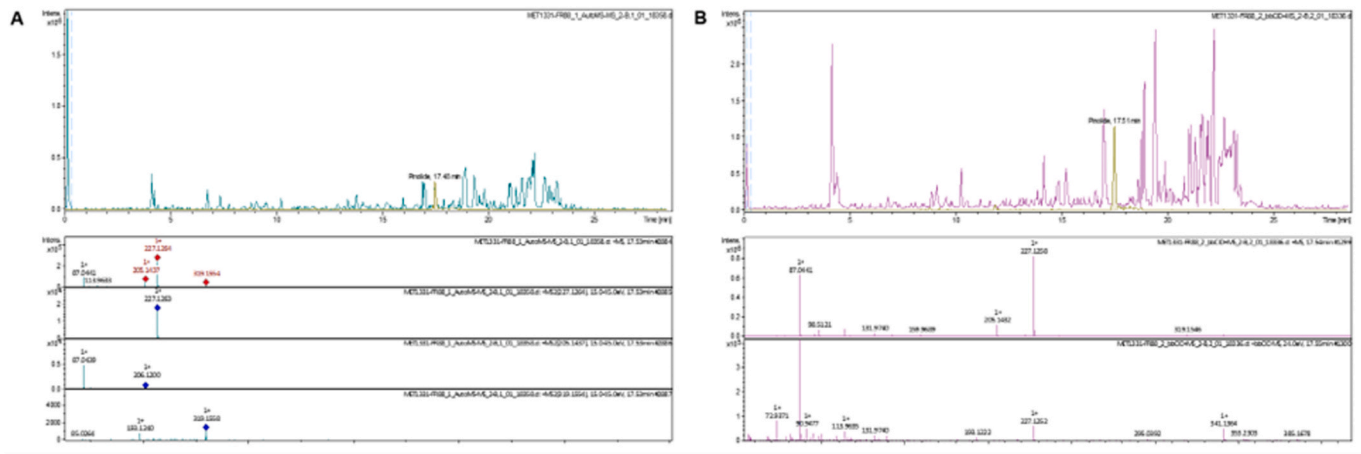


Fig. 1. A) Base peak chromatogram (BPC) and mass spectra recorded in AutoMS/MS mode of *Ascochyta pinodes* FR88 extract; B) BPC and mass spectra recorded in bbCID + MS mode of *A. pinodes* FR88 extract.

ascosonchine, agropyrenol, ascochin, ascochitine, and 5,6-epoxy-pinolidoxin. These compounds have been previously isolated from other *Ascochyta* species. Ascosonchine, identified as (Z)-2-hydroxy-3-(4-pyridyl)-2-propenoic acid, was isolated from the culture filtrate of *A. sonchi*, a pathogen of *Sonchus arvensis*, a widespread perennial weed. This compound exhibited selective herbicidal activity without antibacterial, antifungal, or zootoxic effects [43]. Agropyrenol, a substituted salicylaldehyde, was isolated from *A. agropyrina* var. *nana*, a pathogen of *Elytrigia repens*. Its stereochemistry was established using Mosher's method. Agropyrenol showed the highest phytotoxicity on several weed species, inducing necrotic lesions, while it did not exhibit antimicrobial or zootoxic effects [44]. Ascochin, possessing an unusual substitution pattern confirmed by X-ray diffraction, was isolated from cultures of an endophytic *Ascochyta* sp. [45]. Ascochitine, a polyketide phytotoxin, was initially isolated from *A. pisi* and *A. fabae* and later detected in *Phoma clematidina*. It induced electrolyte leakage and necrotic symptoms in *Clematis* leaf discs, correlating with cultivar susceptibility. The level of ascochitine produced *in vitro* by *P. clematidina* isolates was linked to their virulence. Microscopy revealed that mitochondria and chloroplasts were the primary organelles affected, indicating ascochitine's role in cell death preceding fungal colonization [46]. 5,6-epoxy-pinolidoxin and its derivatives—epipinolidoxin dihydropinolidoxin— were isolated from *A. pinodes* cultured on wheat. Epipinolidoxin and dihydropinolidoxin caused necrosis on pea and bean leaves, while epoxypinolidoxin was inactive in plant assays but, together with epipinolidoxin, showed activity in the brine shrimp toxicity test [10].

Moreover, 19 metabolites that were previously reported from other fungal species are now putatively identified in *A. pinodes*, as listed in Supplementary Table 4. The analysis here reported was particularly interested in detecting several nonenolides, a subclass of macrolides and specialized fungal metabolites. Due to the many possible stereoisomers, some compounds could not be putatively identified at the molecular level but were confidently assigned to the macrolide class based on spectral features. Macrolides are structurally diverse polyketide-derived specialized metabolites characterized by a macrocyclic lactone ring of varying sizes. Defined initially by Woodward in 1957 [47] to describe 14-, 15-, and 16-membered antibiotics, the term has since expanded to include smaller macrocyclic lactones (10–13-membered rings). These compounds are commonly produced by phytopathogenic, marine, and endophytic fungi and exhibit a broad spectrum of biological activities, including antiviral, antibacterial, antifungal, antiparasitic, immunosuppressive, herbicidal, and cytotoxic effects [48].

Exploring the chemical space of *A. pinodes* formed the basis for subsequent plant investigations. In the following experiment, the presence of these compounds was evaluated in pea plants after inoculation, as detailed in section 3.4.

3.4. Detection of fungal specialized metabolites in planta

Although there is extensive literature on *in vitro* studies about fungal specialized metabolites with phytotoxic properties and their roles in plant disease [49,50], only a limited number of studies have specifically investigated the *in vivo* production of these metabolites during plant-fungus interactions [12,15,51]. To our knowledge, this represents the first attempt to identify and quantify specialized metabolites from *A. pinodes* during infection using a metabolomics-based approach. A plant study was designed to determine whether metabolites produced by *A. pinodes* under *in vitro* conditions are also synthesized during host colonization and to assess their potential involvement in disease progression. Sampling was conducted at 24, 48, and 96 hai to monitor metabolite dynamics during early colonization and the progression toward tissue damage, and to capture key stages accompanying symptom development, as necrotic lesions typically appear within this timeframe, as also demonstrated by previous studies [18]. These time points were therefore selected. To monitor fungal metabolite production during infection and examine the corresponding metabolic responses of pea cultivars at different stages, we adopted established extraction protocols utilizing three solvent systems [15,52]. While polar solvents (water/-methanol) primarily capture primary and polar metabolites, such as polyphenols, many fungal specialized metabolites are moderately to highly lipophilic. Thus, the dichloromethane phase was selected for downstream analysis as it is expected to enrich macrolides and related phytotoxic compounds preferentially. Extracted samples were analysed using QTOF mass spectrometry and screened against an in-house database of metabolites identified from *in vitro* cultures of *A. pinodes* (Supplementary Table 4). Of all targeted compounds, only pinolidoxin was detected in infected plant tissues, regardless of sampling time (Fig. 2).

The absence of other metabolites *in planta* may be attributed to several factors: (i) they might not be biosynthesized under *in planta* conditions; (ii) the plant could rapidly detoxify them; or (iii) they may undergo structural modifications or conjugation, rendering them undetectable in their original form. These findings indicate that not all specialized metabolites produced *in vitro* are necessarily synthesized or detectable during host infection. Even if some metabolites are not produced *in planta*, *in vitro* approaches allow exploration of the pathogen's full biosynthetic potential, uncovering a broader chemical space that may include latent or conditionally expressed compounds. This metabolite's repertoire provides a valuable pool of candidates for targeted *in planta* screening for effectors or biomarkers. Thus, comprehensive *in vitro* studies, particularly those employing One Strain Many Compounds (OSMAC) strategies coupled with metabolomics, remain critical [53]. Finally, during host colonization, co-metabolic processes between plant

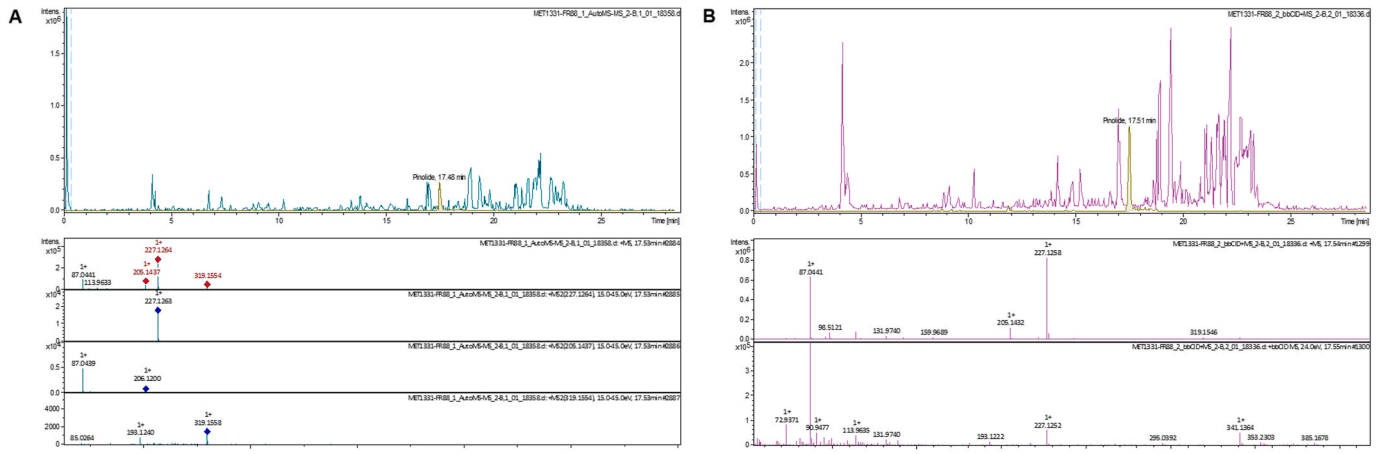


Fig. 2. BPC and mass spectra of pinolidoxin detected in the extract of pea (cv. Radley) inoculated with *Ascochyta pinodes* 48 h after inoculation.

and fungus may generate hybrid or modified compounds not observed under axenic conditions [54,55]. This chemical interplay further complicates the attribution of metabolite origin but also reflects the dynamic nature of the *in planta* metabolic environment, underlining the need to study specific plant-microbe pathosystems using high-throughput screening analytical techniques, thereby overcoming the limitations of *in vitro* or *in vivo* models.

To further confirm the presence and dynamics of pinolidoxin during infection, according to sampling times, a quantitative analysis was performed using the validated QTRAP method. Quantitative results are presented in Table 3, and a representative Multi Reaction Monitoring (MRM) chromatogram is shown in Supplementary Fig. 3.

The analysis confirmed the non-targeted metabolomics findings, revealing that pinolidoxin was quantifiable at all three selected sampling times, with the highest concentrations observed at 48 hai in both pea cultivars: 0.342 ± 0.075 ng/mg in cv. Radley and 0.312 ± 0.132 ng/mg in cv. Messire, followed by a decline at 96 hai. These quantitative trends align with previous targeted proteomics data, which showed upregulation at 48 hai in both cultivars of proteins involved in signal recognition and transduction pathways [18]. Notably, among the proteins upregulated in response to *A. pinodes* were 14-3-3-like proteins, which are known to play a potential role as receptors of fungal toxins [56]. The temporal correlation between the peak in pinolidoxin accumulation and the upregulation of these signalling-related proteins suggests a possible, yet highly speculative, role for pinolidoxin as an effector-like molecule. Indeed, although direct functional evidence is currently lacking, similar infection-stage-specific production patterns have been reported for small-molecule effectors and phytotoxic metabolites in other plant-fungus interactions, where they contribute to host susceptibility by interfering with defence signalling or cellular integrity [49,57,58]. Demonstrating a causal role would require dedicated functional studies, such as gene disruption of biosynthetic pathways, transcriptomic analyses, or bioassays assessing the impact of purified compounds on host responses. Indeed, future investigations should adopt a multi-omics strategy combined with high-throughput phenotyping to deepen our understanding of this pathosystem [13].

Table 3
Concentration of pinolidoxin in wet tissue of pea cultivars 24, 48 and 96 h after infection (hai).

Cultivar	Pinolidoxin (ng/mg)
Radley	
R_{24hai}	$0.057 \pm 0.008^{a*}$
R_{48hai}	0.342 ± 0.075^{b}
R_{96hai}	0.222 ± 0.132^{a}
Messire	
M_{24hai}	0.028 ± 0.017^{c}
M_{48hai}	0.312 ± 0.132^{d}
M_{96hai}	0.066 ± 0.062^{cd}

* Mean ± SD with different letters for each cultivar are significantly different at $p < 0.05$.

3.5. Dysregulated metabolites in inoculated pea cultivars

To fully explore the biological significance of the feature tables generated from LC-MS/MS analysis and to highlight metabolites dysregulated in pea cultivars in response to *A. pinodes* infection, a chemometric analysis was performed. This analysis identified a total of 464 metabolites that were significantly dysregulated (Supplementary Table 6). Among them, 38% were putatively identified, reaching Level B identification [25]. For an additional 16% of features, only the metabolite class (Level C) could be assigned, while 44% remained unidentified or were only annotated by molecular mass (Level D). Based on the selected solvent fraction, 147 dysregulated metabolites were identified in the chloroform extracts and 348 in the methanol/water extracts. Notably, more than half (54%) of the features in the chloroform fraction remained unknown, making biological interpretation and discussion of these results unachievable. Still, all data from this fraction are provided in the Supplementary Materials (Supplementary Figs. 4–7 and Supplementary Table 7). Before discussing the results, some experimental limitations should be considered when interpreting the present findings. The study used two pea cultivars with contrasting responses to *A. pinodes*, allowing identification of genotype-dependent metabolic trends but not capturing the full diversity of resistance mechanisms within the broader pea germplasm. Furthermore, metabolomic analysis was performed exclusively in positive ionization mode. However, this choice was primarily driven by the main objective of this study, the detection and quantification of fungal specialized metabolites produced by *A. pinodes in planta*. Indeed, compounds such as pinolidoxin and structurally related fungal metabolites ionize more efficiently in positive mode [9,10], thereby enhancing sensitivity and reliability in their detection. To address this limitation, a combined untargeted and targeted metabolomics strategy was implemented, facilitating both broad metabolic profiling and sensitive quantification of selected fungal metabolites. However, including negative ionization mode in future studies will provide more comprehensive coverage of the plant metabolome, particularly for negatively charged defense-related compounds. Moreover, the high proportion of unknown features is a common limitation of non-targeted metabolomics. Indeed, fragmentation spectra may match multiple isomers or structural classes, leading to ambiguous or unknown classifications [59]. To overcome these challenges, modern dereplication strategies have emerged, including machine learning, advanced *in silico* fragmentation tools, and molecular networking [60,61]. Moreover, integrating taxonomic information, biological metadata,

and prior experimental knowledge into bioinformatic pipelines can enhance annotation accuracy and improve biological interpretation of dysregulated metabolites [62]. The relatively high proportion of unidentified features observed in the dataset (44%) is consistent with untargeted metabolomics studies but likely also reflects this analytical constraint.

Regarding the analysis of methanol/water extracts from the pea cultivars Messire and Radley, applying a combination of univariate and multivariate analysis enables us to visualize hidden patterns in the data. Initially, comparisons were conducted between inoculated and control plants at each selected sampling time. At 24 hai, no significantly dysregulated metabolites were detected in either Messire or Radley cultivars when compared to their respective controls. In contrast, clear metabolic alterations were observed at a later sampling time. Specifically, significant dysregulation of metabolites was identified in both cultivars at 48 and 96 hai. The complete list of dysregulated metabolites, along with False Discovery Rate (FDR)-adjusted p-values, fold change values (from volcano plot analysis), and Variable Importance for Projection (VIP) scores from the Partial Least Squares Discriminant (PLS-DA) analysis, is provided in Supplementary Table 8. While the normalization process of each data set and the Q2 and R2 values of each PLS-DA model, developed according to the cultural media, are reported in Supplementary Table 5. At 48 hai, volcano plot analysis revealed 17 significantly dysregulated metabolites in cultivar Messire. The most affected superclass was phenylpropanoids and polyketides, particularly the subclasses of flavonoids and isoflavonoids. Moreover, also ferulic acid (M52), a hydroxycinnamic acid, was found to be upregulated in inoculated plants (Fig. 3A). This trend was supported by PLS-DA, which demonstrated clear clustering of the inoculated versus control groups and identified 59 metabolites with a VIP score exceeding the selected threshold of 1.2. Again, phenylpropanoids and polyketides dominated the list, with a significant representation of flavonoids, isoflavonoids, and hydroxycinnamic acids (M90, M117, M125) (Fig. 3B and C). At the same time point (48 hai), a different metabolic response was observed in the resistant cultivar Radley. Here, 28 metabolites were found to be significantly dysregulated, the vast majority being upregulated (Fig. 3D). Notably, the most represented superclass was organic acids and derivatives, with all altered compounds belonging specifically to the amino acids and derivatives class. PLS-DA analysis further confirmed this divergence, with strong separation between groups and 60 metabolites exceeding the VIP threshold, all from the amino acids and derivatives class (Fig. 3E and F).

At 96 hai, both cultivars showed an increased number of dysregulated metabolites, indicating a progression of the plant-pathogen interaction. In Messire, 29 metabolites were significantly altered, as noted in the volcano plot, which was again dominated by phenylpropanoids and polyketides. Flavonoids and isoflavonoids were primarily upregulated, with only two exceptions (M116 and M139) found to be downregulated in inoculated plants (Fig. 4A). PLS-DA results mirrored these findings, with 59 metabolites surpassing the VIP threshold, reinforcing the strong influence of specialized metabolism, especially related to phenylpropanoid-derived compounds (Fig. 4B and C). In Radley, 96 hai, 36 significantly dysregulated metabolites were identified. Interestingly, a shift was observed compared to 48 hai: while amino acids and derivatives remained prominent, there was now substantial representation also from the flavonoids and isoflavonoids classes, indicating a probable late-stage activation of phenylpropanoid metabolism (Fig. 4D). PLS-DA revealed clear group separation and 60 VIP-significant metabolites,

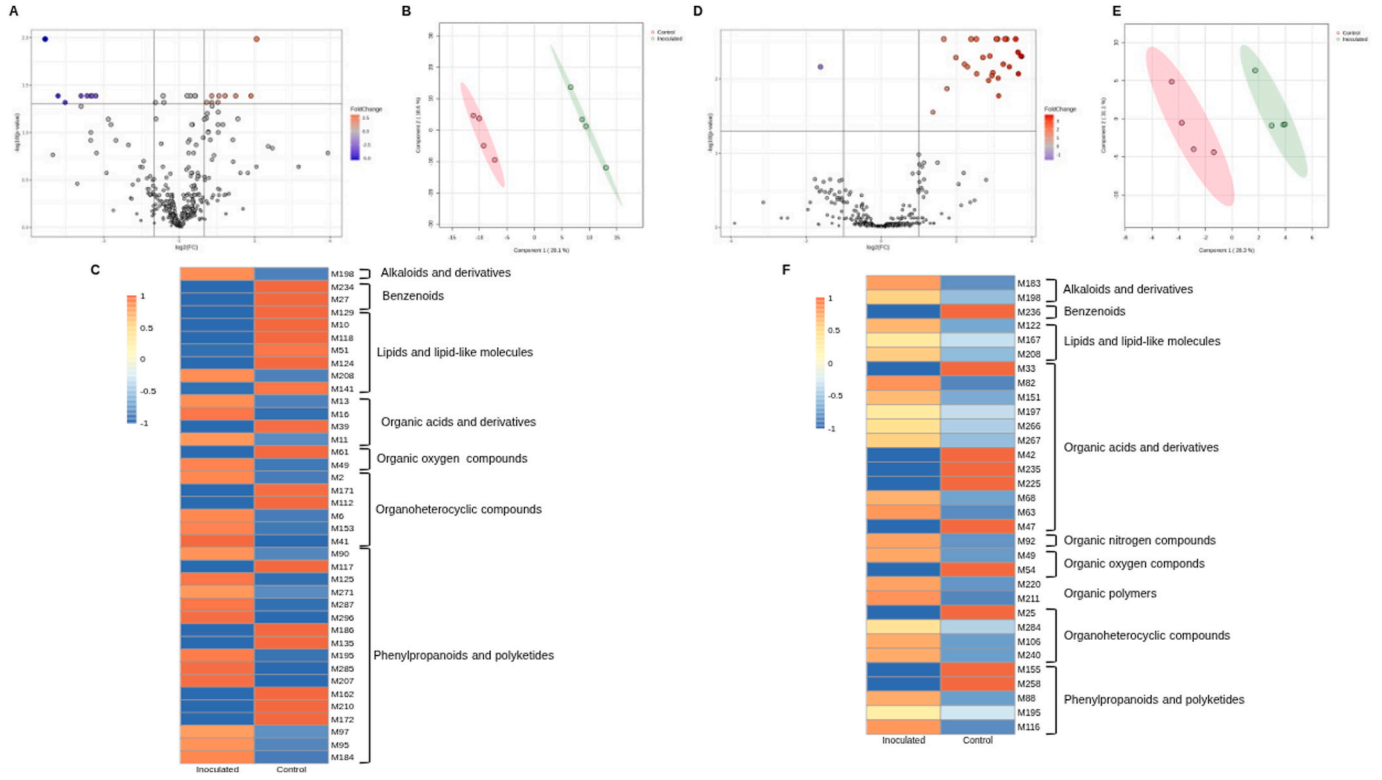


Fig. 3. A) Volcano plot depicting upregulated and downregulated metabolites detected in the methanol/water extracts of inoculated versus control pea (cv. Messire) samples at 48 h after inoculation (hai); B) PLS-DA score plot comparing inoculated (green) and control (red) pea samples (cv. Messire) at 48 hai; C) Heatmap showing metabolites with a VIP score >1.2 in the PLS-DA model for the methanol/water extract of inoculated versus control pea samples at 48 hai; D) Volcano plot depicting upregulated and downregulated metabolites detected in the methanol/water extract of inoculated versus control pea (cv. Radley) samples at 48 hai; E) PLS-DA score plot comparing inoculated (green) and control (red) pea samples (cv. Radley) at 48 hai; F) Heatmap showing metabolites with a VIP score >1.2 in the PLS-DA model for the methanol/water extract of inoculated versus control pea samples at 48 h post-inoculation. (For interpretation of the references to colour in this figure legend, the reader is referred to the Web version of this article.)

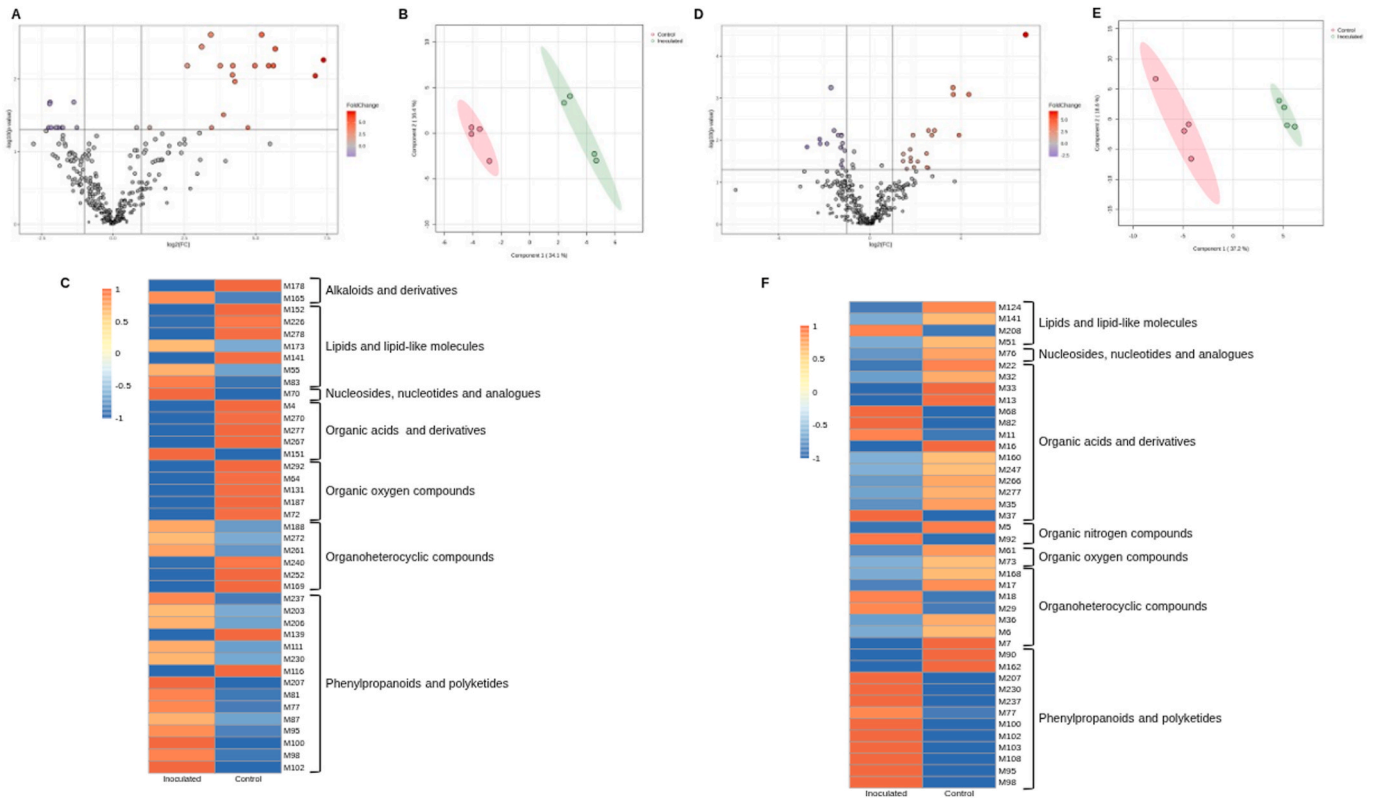


Fig. 4. A) Volcano plot depicting upregulated and downregulated metabolites detected in the methanol/water extracts of inoculated versus control pea (cv. Messire) samples at 96 h after inoculation (hai); B) PLS-DA score plot comparing inoculated (green) and control (red) pea samples (cv. Messire) at 96 hai; C) Heatmap showing metabolites with a VIP score >1.2 in the PLS-DA model for the methanol/water extract of inoculated versus control pea samples at 96 hai; D) Volcano plot depicting upregulated and downregulated metabolites detected in the methanol/water extract of inoculated versus control pea (cv. Radley) samples at 96 hai; E) PLS-DA score plot comparing inoculated (green) and control (red) pea samples (cv. Radley) at 96 hai; F) Heatmap showing metabolites with a VIP score >1.2 in the PLS-DA model for the methanol/water extract of inoculated versus control pea samples at 48 h post-inoculation. (For interpretation of the references to colour in this figure legend, the reader is referred to the Web version of this article.)

again pointing to two majors affected superclasses: phenylpropanoids and polyketides, as well as organic acids and their derivatives (Fig. 4E and F). Within the phenylpropanoids, most compounds were upregulated; however, metabolite M90, putatively annotated as a hydroxycinnamic acid derivative, was downregulated. Within the organic acids and derivatives, nearly all dysregulated metabolites continued to belong to the amino acids and derivatives class.

To explore the temporal evolution of metabolite dysregulation in response to *A. pinodes* infection, Principal Component Analysis (PCA) and univariate (ANOVA) analyses were conducted using MetaboAnalyst, focusing exclusively on the inoculated plants. In cultivar Messire, PCA revealed three distinct clusters corresponding to the sampling times, as shown in the score plot (Fig. 5A). Samples collected at 48 hai and 96 hai were separated along PC1, while both were clearly distinguished from those at 24 hai along PC2. The top 20 metabolites contributing to the separation among time points are presented in Supplementary Fig. 8A. Among them, the most represented superclass was phenylpropanoids and polyketides, with six metabolites all belonging to the subclasses of flavonoids and isoflavonoids. ANOVA identified 12 significant metabolites (FDR-adjusted $p < 0.05$), primarily belonging to two superclasses: organic acids and derivatives, specifically amino acids and derivatives, and phenylpropanoids and polyketides, particularly flavonoids and isoflavonoids (Fig. 5C). Interestingly, amino acid levels were highest at 24 hai but decreased at 48 hai and 96 hai, suggesting a metabolic shift. In contrast, the relative abundance of flavonoids and isoflavonoids increased significantly at 96 hai, indicating a delayed activation of specialized metabolism, potentially linked to plant defense. Similarly, in cultivar Radley, PCA also highlighted clear temporal clustering, with 96 hai samples forming a distinct group in the lower left quadrant of the score plot, separated from 48 hai samples along PC1 and from 24 hai samples along PC2 (Fig. 5B). The top 20 contributing metabolites to this separation are shown in Supplementary Fig. 8B. As in Messire, the most represented superclass among these metabolites was phenylpropanoids and polyketides. Apart from one coumarin (M67), all other significant compounds belonged to the flavonoids and isoflavonoids subclasses. ANOVA in Radley revealed 10 significantly dysregulated metabolites (FDR-adjusted $p < 0.05$), most of which were flavonoids and isoflavonoids. Their relative abundance increased over time, being higher at 96 hai (Fig. 5D).

Finally, a comparative analysis of the inoculated plants from both cultivars was conducted to uncover potential metabolic differences in their responses to *A. pinodes* infection. Both the volcano plot and PLS-DA analyses revealed a clear metabolic distinction between the two cultivars. A comprehensive list of dysregulated metabolites, complete with FDR-adjusted p-values, fold changes from the volcano plot, and VIP scores from the PLS-DA, is available in Supplementary Table 4. Although metabolic differences were observed at all three sampling times, the most pronounced divergence occurred 48 hai. At this point, the majority of dysregulated metabolites belonged to the superclass of phenylpropanoids and polyketides, with a strong enrichment in flavonoids and hydroxycinnamic acids. All of these metabolites were upregulated in the Messire cultivar, suggesting an intensified phenolic response. Only a single flavonoid, putatively identified as isorhamnetin 3-galactoside, was found to be downregulated in Messire (Fig. 6).

Flavonoids also emerged as the most consistently affected class at the other two time points (24 hai and 96 hai), although a greater proportion of unknown metabolites was detected (Supplementary Fig. 9). This consistent enrichment of flavonoid-related compounds underscores

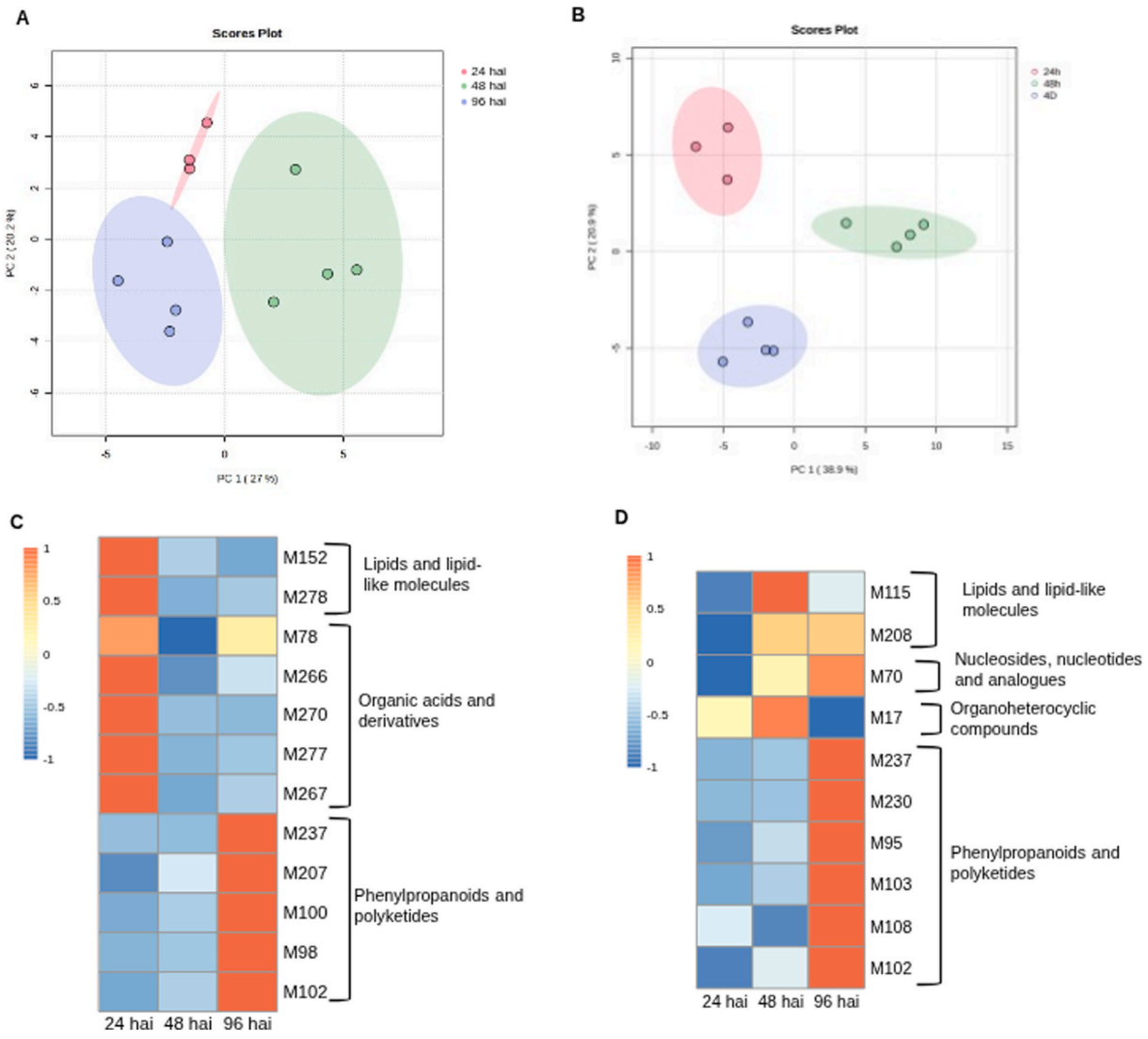


Fig. 5. A) PCA score plot comparing the MeOH extract of inoculated pea (cv. Messire) at 24 h after inoculation (hai) (red), 48 hai (green) and 96h (blue) after inoculation; B) PCA score plot comparing the MeOH extract of inoculated pea (cv. Radley) at 24 hai (red), 48 hai (green) and 96 hai (blue) after inoculation; C) Heatmap displaying identified metabolites find to be significantly (ANOVA, $p < 0.05$) altered in the MeOH extract of pea (cv. Messire) at 24 hai, 48hai and 96 hai after inoculation; D) Heatmap displaying identified metabolites find to be significantly (ANOVA, $p < 0.05$) altered in the MeOH extract of pea (cv. Radley) at 24 hai, 48 hai and 96 hai after inoculation. (For interpretation of the references to colour in this figure legend, the reader is referred to the Web version of this article.)

their potential role as key players in cultivar-specific defense responses against *A. pinodes*.

Collectively, these observations demonstrate temporal and genotype-dependent patterns in the metabolomic response to *A. pinodes* infection. However, it is important to emphasize that the associations described here are correlative rather than causal. Indeed, these differential metabolic responses could reflect downstream consequences of distinct immune activation pathways, secondary effects of varying infection severity, or metabolic adjustments to pathogen-induced stress rather than primary resistance mechanisms. To establish causality, functional validation through gene expression analyses of key biosynthetic pathways, reverse genetics approaches, metabolic perturbation experiments together with multiomic analysis and targeted metabolomics would be required. Nevertheless, these correlative findings provide valuable insights into the metabolic landscape of host-pathogen interactions and identify potential biomarkers for screening resistance or susceptibility. Indeed, current studies are advancing the understanding of legume immune systems, particularly under attack by fungi, highlighting the multi-layered defense mechanisms [63].

Messire showed an early activation of specialized metabolism, especially in flavonoids, isoflavonoids, and hydroxycinnamic acid. In legumes, flavonoids and isoflavonoids play crucial roles in plant defense, accumulating before, during, and after microbial attack [64]. Nevertheless, their biological functions are more complex. Indeed, certain isoflavonoids act as chemoattractants, growth promoters, and inducers of nodulation genes in symbiotic bacteria such as *Rhizobium* and *Bradyrhizobium* [65]. For instance, flavonoids such as naringenin, kaempferol, and quercetin act as signalling molecules that can even induce virulence genes in *Agrobacterium tumefaciens* and *Pseudomonas syringae* [66]. However, the outcome of these interactions is often species-specific: while some flavonoids stimulate germination of fungal spores, others, like phloretin, naringenin, apigenin, daidzein, and quercetin, induce resistance against *Fusarium oxysporum* or *Colletotrichum gloeosporioides* [67,68]. Similarly, in chickpea infected by *A. rabiei*, metabolomic profiling revealed that flavonoid biosynthesis is differentially activated depending on the genotype. In moderately resistant accessions, flavonoids may contribute to an effective defense, while in susceptible ones, the fungus may use this pathway to its advantage [69]. So, considering the context-specific nature of their effects, further investigations are needed. Phenolic acids are known to

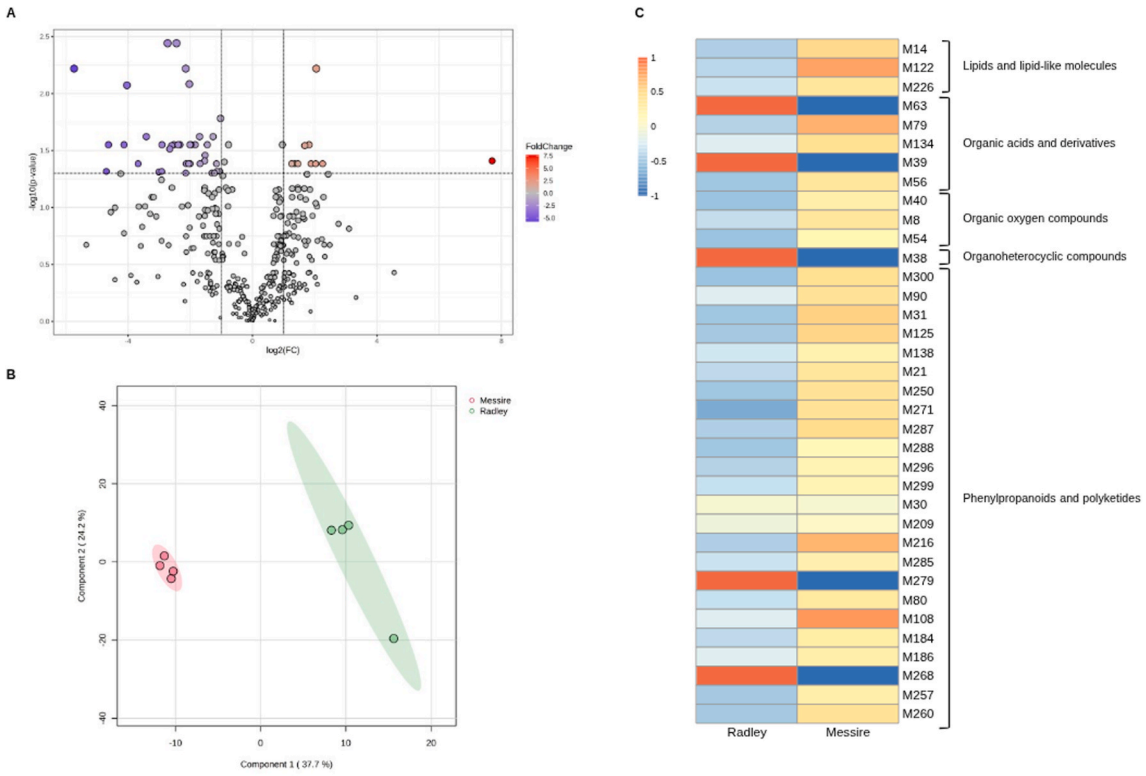


Fig. 6. A) Volcano plot depicting upregulated and downregulated metabolites detected in the MeOH extract of inoculated pea cv. Radley versus cv. Messire at 48 h after inoculation (hai); B) PLS-DA score plot comparing inoculated pea cv. Radley (green) and cv. Messire (red) at 48 hai; C) Heatmap showing metabolites with a VIP score >1.2 in the PLS-DA model for the methanol/water extract of pea cv. Radley and cv. Messire samples 48 hai. (For interpretation of the references to colour in this figure legend, the reader is referred to the Web version of this article.)

induce *nod* genes in rhizobia, *vir* genes in *A. tumefaciens*, and participate in the establishment of symbiosis by inducing fungal genes, such as *GmGin1*. They also play a role in defense against soil-borne pathogens, impacting the microbial ecology of the rhizosphere [70,71]. Among phenolic acids, metabolites such as ferulic acid have demonstrated antimicrobial activity and are involved in triggering plant immune responses, including reactive oxygen species (ROS) production, cell wall reinforcement, defense hormone signalling, and stomatal immunity. However, the mechanisms by which hydroxycinnamic acids contribute to defense remain complex and not fully understood [35]. Nonetheless, specific phenolic acids can have adverse effects on plant resistance. For instance, cinnamic acid has been shown to enhance *Fusarium* pathogenicity by inhibiting plant defense enzymes and compromising root immunity [72].

The resistant pea cv. Radley exhibited a more pronounced early upregulation of amino acid derivatives, probably indicating a distinctive defense strategy linked to enhanced primary metabolism. Indeed, previous studies highlighted amino acids play a critical dual role in plant–pathogen interactions, acting both as metabolic intermediates and signalling molecules that shape systemic immune responses. Specific amino acids, such as glutamate, proline, γ-aminobutyric acid (GABA), β-aminobutyric acid (BABA), and pipecolic acid, are involved in modulating defense pathways [73]. In parallel, amino acid transporters regulate the cellular distribution of amino acids, influencing either plant defense or pathogen nutrition depending on tissue and substrate specificity. There is growing evidence for the coordinated regulation of amino acid and sugar transporters, further highlighting their strategic roles in controlling nutrient flux at the host–pathogen interface [73]. Ultimately, the here presented findings regarding metabolic dysregulation of amino acids and their derivatives in the resistant pea cultivar Radley align with previous targeted proteomics studies of the pea-*A. pinodes* pathosystem. These studies indicate that resistant pea cultivars exhibit increased levels of proteins involved in energy and amino acid metabolism, which likely support the energetic requirements of resistance mechanisms [18]. Similarly, Fondevilla et al. [74] observed upregulation of genes related to protein synthesis and maturation in a pea accession resistant to *A. pinodes* [74,75].

The distinct metabolic profiles observed may indicate extensive reprogramming of central metabolic pathways during infection, involving trade-offs between carbon and nitrogen metabolism. Strong activation of phenylpropanoid metabolism in the susceptible cv. Messire suggests significant carbon allocation to specialized metabolite synthesis. Although this response is typically linked to plant immune function, it may represent a delayed or ineffective strategy that does not sufficiently restrict pathogen progression [76]. Conversely, the resistant cv. Radley exhibited early and sustained upregulation of amino acids and their derivatives, indicating a shift toward nitrogen metabolism and reinforcement of primary metabolism. This metabolic reprogramming may fulfil the energetic and biosynthetic requirements of rapid, coordinated defense responses [77]. The balance between phenylpropanoid flux and nitrogen metabolism has been proposed as a critical determinant of resistance outcomes, reflecting alternative strategies of resource allocation during plant–pathogen interactions [78]. Nevertheless, as previously mentioned, this correlation should be validated.

4. Conclusion

This study provides the first *in vivo* metabolomics-based evidence of *Ascochyta pinodes* specialized metabolite production during pea infection, identifying pinolidoxin as the unique fungal compound consistently detected and quantified in infected plant tissues under our experimental conditions. Findings here presented suggest that pinolidoxin may act as an effector molecule, potentially facilitating early stages of infection, and thus could be used as a potential biomarker for

the early detection of the infection. Our non-targeted metabolomics approach revealed cultivar-specific metabolic dysregulation in response to infection. The susceptible cv. Messire exhibited a strong upregulation of flavonoids and isoflavonoids; conversely, the cv. Radley displayed increased levels of amino acids and their derivatives, suggesting differences in the defense strategy based on adjustments to primary metabolism, which underscores these metabolites as biomarkers for disease resistance in peas. Future metabolomic studies should focus on validation through targeted approaches that concentrate on the most dysregulated compounds. Nevertheless, the high number of unknown metabolites, especially those from the chloroform extract, raises important questions, as they might come from the fungus and be part of its unknown chemical space. Identifying these compounds will help to gain a better understanding of how the fungus and plant interact during infection. Looking ahead, future investigations should be conducted across a wide range of pea germplasm collections to enable a more comprehensive evaluation of host-dependent metabolic responses. In addition, integrating dual-polarity acquisition modes and applying complementary extraction strategies to improve metabolite coverage, also including MS/MS-driven GNPS molecular networking and larger spectral libraries, would facilitate deeper characterization of the metabolic landscape underlying the *P. sativum-A. pinodes* interaction. Finally, adopting an integrated multi-omics strategy could help to elucidate the intricate chemical dialogue between the host and pathogen, resulting in the identification of virulence strategies. Such multifaceted approaches can support the identification of metabolite-based markers associated with resistance, thereby facilitating their integration into breeding programs to select disease-tolerant pea cultivars. Additionally, understanding *Ascochyta*-derived metabolite dynamics during infection may inform future strategies for disease biocontrol and management, ultimately reducing reliance on synthetic broad-spectrum fungicides in pea cropping systems.

CRediT authorship contribution statement

Pierluigi Reveglia: Conceptualization, Data curation, Investigation, Methodology, Writing – original draft. **Sara Rodriguez-Mena:** Data curation, Investigation, Visualization, Writing – review & editing. **José E. Yuste:** Investigation, Methodology. **Lucia Lecce:** Investigation, Methodology. **Diego Rubiales:** Funding acquisition, Supervision, Writing – review & editing. **Eleonora Barilli:** Investigation, Methodology, Validation, Writing – review & editing.

Declaration of competing interest

The authors declare that they have no known competing financial interests or personal relationships that could have appeared to influence the work reported in this paper.

Acknowledgements

We acknowledge Professors Alessio Cimmino and Marco Masi at University of Naples, Federico II for supplying pinolidoxin and diacetylpinolidoxin. This work was funded by the Spanish Ministry of Science and Innovation, project PID2023-146215OB-I00 (MCIN/AEI/10.13039/501100011033) and the Horizon Europe project BELIS (num. 101081878).

Appendix A. Supplementary data

Supplementary data to this article can be found online at https://doi.org/10.1016/j.pmpp.2026.103244.

Data availability

All data are available in the manuscript and supplementary material. Raw mass spectrometry data will be made available on request.

References

[1] N. Windsor, L. Boatwright, R. Boyles, W. Bridges, D. Rubiales, D. Thavarajah, Characterizing dry pea (*Pisum sativum* L.) for improved nutritional traits and the potential for biofortification, Legum. Sci. 6 (2024) e250, https://doi.org/10.1002/leg3.250.
[2] D. Rubiales, E. Barilli, N. Rispail, Breeding for biotic stress resistance in pea, Agriculture 13 (2023) 1825, https://doi.org/10.3390/agriculture13091825.
[3] K. Stałanowska, J. Szablińska-Piernik, A. Pszczółkowska, V. Railean, M. Wasicki, P. Pomastowski, L.P. Lahuta, A. Okorski, Antifungal properties of bio-AgNPs against *D. pinodes* and *F. avenaceum* infection of pea (*Pisum sativum* L.) seedlings, Int. J. Mol. Sci. 25 (2024) 4525, https://doi.org/10.3390/ijms25084525.
[4] B. Tivoli, S. Banniza, Comparison of the epidemiology of ascochyta blights on grain legumes, in: B. Tivoli, A. Baranger, F.J. Muehlbauer, B.M. Cooke, B. M (Eds.), Ascochyta Blights of Grain Legumes, Springer, Dordrecht, 2007, pp. 59–76.
[5] M.A. Castillejo, M. Curto, S. Fondevilla, D. Rubiales, J.V. Jorrín, Two-dimensional electrophoresis based proteomic analysis of the pea (*Pisum sativum*) in response to *Mycosphaerella pinodes*, J. Agric. Food Chem. 58 (2010) 12822–12832, https://doi.org/10.1021/jf1036917.
[6] E. Carrillo-Perdomo, D. Rubiales, A. Pérez-De-Luque, S. Fondevilla, Characterization of mechanisms of resistance against *Didymella pinodes* in *Pisum* spp, Eur. J. Plant Pathol. 135 (2013) 761–769, https://doi.org/10.1007/s10658-012-0116-0.
[7] W. Kim, W. Chen, Phytotoxic metabolites produced by legume-associated *Ascochyta* and its related genera in the *Dothideomycetes*, Toxins 11 (2019) 627, https://doi.org/10.3390/toxins11110627.
[8] F.J. Agudo-Jurado, P. Reveglia, D. Rubiales, A. Evidente, E. Barilli, Status of phytotoxins isolated from necrotrophic fungi causing diseases on grain legumes, Int. J. Mol. Sci. 24 (2023) 5116, https://doi.org/10.3390/ijms24065116.
[9] A. Evidente, R. Lanzetta, R. Capasso, M. Vurro, A. Bottalico, Pinolidoxin, a phytotoxic nonenolide from *Ascochyta pinodes*, Phytochemistry 34 (1993) 999–1003, https://doi.org/10.1016/S0031-9422(00)90702-7.
[10] A. Cimmino, A. Andolfi, S. Fondevilla, M.A. Abouzeid, D. Rubiales, A. Evidente, Pinolide, a new nonenolide produced by *Didymella pinodes*, the causal agent of *Ascochyta* blight on *Pisum sativum*, J. Agric. Food Chem. 60 (2012) 5273–5278, https://doi.org/10.1021/jf300824d.
[11] W. Kim, T.L. Peever, J.J. Park, C.M. Park, D.R. Gang, M. Xian, J.A. Davidson, A. Infantino, W.J. Keiser, W. Chen, Use of metabolomics for the chemotaxonomy of legume-associated *Ascochyta* and allied genera, Sci. Rep. 6 (2016) 20192, https://doi.org/10.1038/srep20192.
[12] I. Buckel, L. Andernach, A. Schüffler, M. Piepenbring, T. Opatz, E. Thines, Phytotoxic dioxolanones are potential virulence factors in the infection process of *Guignardia bidwellii*, Sci. Rep. 7 (2017) 1–7, https://doi.org/10.1038/s41598-017-09157-6.
[13] B. Ball, M. Langille, J. Geddes-McAlister, Fun (gi) omics: advanced and diverse technologies to explore emerging fungal pathogens and define mechanisms of antifungal resistance, mBio 11 (2020) e01020, https://doi.org/10.1128/mbio.01020-20, 01020.
[14] F.R. Castro-Moretti, I.N. Gentzel, D. Mackey, A.P. Alonso, Metabolomics as an emerging tool for the study of plant-pathogen interactions, Metabolites 10 (2020) 52, https://doi.org/10.3390/metabo10020052.
[15] P. Reveglia, R. Billones-Baaijens, J. Millera Niem, M. Masi, A. Cimmino, A. Evidente, S. Savocchia, Production of phytotoxic metabolites by Botryosphaeriaceae in naturally infected and artificially inoculated grapevines, Plants 10 (2021) 802, https://doi.org/10.3390/plants10040802.
[16] G. Desalegn, R. Turetschek, H.P. Kaul, S. Wienkoop, Microbial symbionts affect *Pisum sativum* proteome and metabolome under *Didymella pinodes* infection, J. Proteonom. 143 (2016) 173–187, https://doi.org/10.1016/j.jprot.2016.03.018.
[17] N. Ranjbar Sistani, H.-P. Kaul, G. Desalegn, S. Wienkoop, Rhizobium impacts on seed productivity, quality, and protection of *Pisum sativum* upon disease stress caused by *Didymella pinodes*: phenotypic, proteomic, and metabolomic traits, Front. Plant Sci. 8 (2017) 1961, https://doi.org/10.3389/fpls.2017.01961.
[18] M.A. Castillejo, S. Fondevilla-Aparicio, C. Fuentes-Almagro, D. Rubiales, Quantitative analysis of target peptides related to resistance against *Ascochyta* blight (*Peyronellaea pinodes*) in pea, J. Proteome Res. 19 (2020) 1000–1012, https://doi.org/10.1021/acs.jproteome.9b00365.
[19] E. Barilli, P. Reveglia, F.J. Agudo-Jurado, V. Cañete García, A. Cimmino, A. Evidente, D. Rubiales, Comparative analysis of secondary metabolites produced by *Ascochyta fabae* under *in vitro* conditions and their phytotoxicity on the primary host, *Vicia faba*, and related legume crops, Toxins 15 (2023) 693, https://doi.org/10.3390/toxins15120693.
[20] S. Fondevilla, J. Cubero, D. Rubiales, Response to *Mycosphaerella pinodes* in a germplasm collection of *Pisum* spp, Plant Breed. 124 (2005) 313–315, https://doi.org/10.1111/j.1439-0523.2005.01104.x.
[21] E. Barilli, M.J. Cobos, D. Rubiales, Clarification on host range of *Didymella pinodes* the causal agent of pea Ascochyta blight, Front. Plant Sci. 7 (2016) 592, https://doi.org/10.3389/fpls.2016.00592.
[22] J.M. Kraft, B. Dunne, D. Goulden, S. Armstrong, A search for resistance in peas to *Mycosphaerella pinodes*, Plant Dis. 82 (1998) 251–253, https://doi.org/10.1094/PDIS.1998.82.2.251.
[23] C. Roger, B. Tivoli, Spatio-temporal development of pycnidia and perithecia and dissemination of spores of *Mycosphaerella pinodes* on pea (*Pisum sativum*), Plant Pathol. 45 (1996) 518–528, https://doi.org/10.1046/j.1365-3059.1996.d01-139.x.
[24] H. Tsugawa, T. Cajka, T. Kind, Y. Ma, B. Higgins, K. Ikeda, M. Kanazawa, J. VanderGheynst, O. Fiehn, M. Arita, MS-DIAL: data-independent MS/MS

deconvolution for comprehensive metabolome analysis, Nat. Methods 12 (2015) 523–526, https://doi.org/10.1038/nmeth.3393.
[25] S. Alseekh, A. Aharoni, Y. Brotman, K. Contrepois, J. D'Auria, J. Ewald, J.C. Ewald, P.D. Fraser, P. Giavalisco, R.D. Hall, Mass spectrometry-based metabolomics: a guide for annotation, quantification and best reporting practices, Nat. Methods 18 (2021) 747–756, https://doi.org/10.1038/s41592-021-01197-1.
[26] E.F. Poynton, J.A. Van Santen, M. Pin, M.M. Contreras, E. McMann, J. Parra, B. Showalter, L. Zaroubi, K.R. Duncan, R.G. Linington, The natural products Atlas 3.0: extending the database of microbially derived natural products, Nucleic Acids Res. 53 (2025) 691–699, https://doi.org/10.1093/nar/gkae1093.
[27] Z. Pang, J. Chong, G. Zhou, D.A. De Lima Morais, L. Chang, M. Barrette, C. Gauthier, P.-É. Jacques, S. Li, J. Xia, MetaboAnalyst 5.0: narrowing the gap between raw spectra and functional insights, Nucleic Acids Res. 1 (2021) 388–396, https://doi.org/10.1093/nar/gkab382.
[28] M. Farrés, S. Platikanov, S. Tsakovski, R. Tauler, Comparison of the variable importance in projection (VIP) and of the selectivity ratio (SR) methods for variable selection and interpretation, J. Chem. 29 (2015) 528–536, https://doi.org/10.1002/cem.2736.
[29] R. Kolde, M.R. Kolde, Package 'pheatmap, R package 1 (2015) 790, https://doi.org/10.32614/CRAN.package.pheatmap.
[30] H. Wickham, Advanced R, second ed., Chapman and Hall/CRC, New York, 2019.
[31] C. Osterhage, R. Kaminsky, G.M. König, A.D. Wright, Ascosalipyrrolidinone a, an antimicrobial alkaloid, from the obligate marine fungus *Ascochyta salicorniae*, J. Org. Chem. 65 (2000) 6412–6417, https://doi.org/10.1021/jo000307g.
[32] S.F. Seibert, E. Eguereva, A. Krick, S. Kehraus, E. Voloshina, G. Raabe, J. Fleischhauer, E. Leistner, M. Wiese, H. Prinz, Polyketides from the marine-derived fungus *Ascochyta salicorniae* and their potential to inhibit protein phosphatases, Org. Biomol. Chem. 4 (2006) 2233–2240, https://doi.org/10.1039/B601386D.
[33] A. Fürstner, K. Radkowski, C. Wirtz, R. Goddard, C.W. Lehmann, R. Mynott, Total syntheses of the phytotoxic lactones herbarumin I and II and a synthesis-based solution of the pinolidoxin puzzle, J. Am. Chem. Soc. 124 (2002) 7061–7069, https://doi.org/10.1021/ja020238i.
[34] D. Liu, S.A. Kozmin, Synthesis of (−)-pinolidoxin: divergent synthetic strategy exploiting a common silacyclic precursor, Org. Lett. 4 (2002) 3005–3007, https://doi.org/10.1021/ol026433j.
[35] J. Bi, M. Chen, P. Nie, Y. Liu, J. Liu, Y. Du, Stereoselective total synthesis of natural decanolides bellidisin C and pinolidoxin, Molecules 29 (2024) 5500, https://doi.org/10.3390/molecules29235500.
[36] J. Guo, T. Huan, Comparison of full-scan, data-dependent, and data-independent acquisition modes in liquid chromatography–mass spectrometry based untargeted metabolomics, Anal. Chem. 92 (2020) 8072–8080, https://doi.org/10.1021/acs.analchem.9b05135.
[37] H.P. Benton, J. Ivanisevic, N.G. Mahieu, M.E. Kurczy, C.H. Johnson, L. Franco, D. Rinehart, E. Valentine, H. Gowda, B.K. Ubhi, Autonomous metabolomics for rapid metabolite identification in global profiling, Anal. Chem. 87 (2015) 884–891, https://doi.org/10.1021/ac5025649.
[38] H.L. Röst, G. Rosenberger, P. Navarro, L. Gillet, S.M. Miladinović, O.T. Schubert, W. Wolski, B.C. Collins, J. Malmström, L. Malmström, OpenSWATH enables automated, targeted analysis of data-independent acquisition MS data, Nat. Biotechnol. 32 (2014) 219–223, https://doi.org/10.1038/nbt.2841.
[39] X. Zhu, Y. Chen, R. Subramanian, Comparison of information-dependent acquisition, SWATH, and MSAll techniques in metabolite identification study employing ultrahigh-performance liquid chromatography–quadrupole time-of-flight mass spectrometry, Anal. Chem. 86 (2014) 1202–1209, https://doi.org/10.1021/ac403385y.
[40] D. Siegel, A.C. Meinema, H. Permentier, G. Hopfgartner, R. Bischoff, Integrated quantification and identification of aldehydes and ketones in biological samples, Anal. Chem. 86 (2014) 5089–5100, https://doi.org/10.1021/ac500810r.
[41] A.C. Schrimpe-Rutledge, S.G. Codreanu, S.D. Sherrod, J.A. McLean, Untargeted metabolomics strategies-challenges and emerging directions, J. Am. Soc. Mass Spectrom. 27 (2016) 1897–1905, https://doi.org/10.1007/s13361-016-1469-y.
[42] V. Lindemann, J. Schmidt, B. Cramer, H.U. Humpf, Detection of mycotoxins in highly matrix-loaded house-dust samples by QTOF-HRMS, IM-QTOF-HRMS, and TQMS: advantages and disadvantages, Anal. Chem. 94 (2022) 4209–4217, https://doi.org/10.1021/acs.analchem.1c04254.
[43] A. Evidente, A. Andolfi, M.A. Abouzeid, M. Vurro, M.C. Zonno, A. Motta, Ascosonchine, the enol tautomer of 4-pyridylpyruvic acid with herbicidal activity produced by *Ascochyta sonchi*, Phytochemistry 65 (2004) 475–480, https://doi.org/10.1016/j.phytochem.2003.09.016.
[44] A. Andolfi, A. Cimmino, M. Vurro, A. Berestetskiy, C. Troise, M.C. Zonno, A. Motta A. Evidente, Agropyrenol and agropyrenal, phytotoxins from *Ascochyta agropyrina* var. *nana*, a fungal pathogen of *Elitrigia repens*, Phytochemistry 79 (2012) 102–108, https://doi.org/10.1016/j.phytochem.2012.03.010.
[45] K. Krohn, I. Kock, B. Elsässer, U. Flörke, B. Schulz, S. Draeger, G. Pescitelli, S. Antus, T. Kurtán, Bioactive natural products from the endophytic fungus *Ascochyta* sp. from *Meliotus dentatus*–configurational assignment by solid-state CD and TDDFT calculations, Eur. J. Org. Chem. 7 (2007) 1123–1129, https://doi.org/10.1002/ejoc.200600907.
[46] G. Smith, M. Munro, B. Fineran, A. Cole, Evidence for the involvement of ascochitine in phoma leafspot-wilt disease of *Clematis*, Physiol. Mol. Plant Pathol. 45 (1994) 333–348, https://doi.org/10.1016/S0885-5765(05)80063-3.
[47] R.B. Woodward, Struktur und biogenese der makrolide, Angew. Chem. 69 (1957) 50–58, https://doi.org/10.1002/ange.19570690109.
[48] A. Evidente, Fungal bioactive macrolides, Nat. Prod. Rep. 39 (2022) 1591–1621, https://doi.org/10.1039/D2NP00025C.
[49] J. Mapuranga, J. Chang, L. Zhang, N. Zhang, W. Yang, Fungal secondary metabolites and small RNAs enhance pathogenicity during plant-fungal pathogen interactions, J. Fungi 9 (2022) 4, https://doi.org/10.3390/jof9010004.
[50] T.A.N. Nguyen, T. Higa, A. Shiina, Y.D. Utami, K. Hiruma, Exploring the roles of fungal-derived secondary metabolites in plant-fungal interactions, Physiol. Mol. Plant Pathol. 125 (2023) 102021, https://doi.org/10.1016/j.pmpp.2023.102021.
[51] Y. Li, Z. Gai, C. Wang, P. Li, B. Li, Identification of mellein as a pathogenic substance of *Botryosphaeria dothidea* by UPLC-MS/MS analysis and phytotoxic bioassay, J. Agric. Food Chem. 69 (2021) 8471–8848, https://doi.org/10.1021/acs.jafc.1c03249.
[52] J. Kang, L. David, Y. Li, J. Cang, S. Chen, Three-in-one simultaneous extraction of proteins, metabolites and lipids for multi-omics, Front. Genet. 12 (2021) 635971, https://doi.org/10.3389/fgene.2021.635971.
[53] R. Pan, X. Bai, J. Chen, H. Zhang, H. Wang, Exploring structural diversity of microbe secondary metabolites using OSMAC strategy: a literature review, Front. Microbiol. 10 (2019) 294, https://doi.org/10.3389/fmicb.2019.00294.
[54] T. Pusztahelyi, I.J. Holb, I. Pócsi, Secondary metabolites in fungus-plant interactions, Front. Plant Sci. 6 (2015) 573, https://doi.org/10.3389/fpls.2015.00573.
[55] B. Ökmen, G. Doehlemann, Inside plant: biotrophic strategies to modulate host immunity and metabolism, Curr. Opin. Plant Biol. 20 (2014) 19–25, https://doi.org/10.1016/j.pbi.2014.03.011.
[56] R.J. Ferl, 14-3-3 proteins and signal transduction, Annu. Rev. Plant Biol. 47 (1996) 49–73, https://doi.org/10.1146/annurev.arplant.47.1.49.
[57] A. Pradhan, S. Ghosh, D. Sahoo, G. Jha, Fungal effectors, the double edge sword of phytopathogens, Curr. Genet. 67 (2021) 27–40, https://doi.org/10.1007/s00294-020-01118-3.
[58] L. Rodriguez-Moreno, M.K. Ebert, M.D. Bolton, B.P. Thomma, Tools of the crook-infection strategies of fungal plant pathogens, Plant J. 93 (2018) 664–674, https://doi.org/10.1111/tpj.13810.
[59] W. Bittremieux, M. Wang, P.C. Dorrestein, The critical role that spectral libraries play in capturing the metabolomics community knowledge, Metabolomics 18 (2022) 94, https://doi.org/10.1007/s11306-022-01947-y.
[60] P.-M. Allard, T. Péresse, J. Bisson, K. Gindro, L. Marcourt, V.C. Pham, F. Roussi, M. Litaudon, J.-L. Wolfender, Integration of molecular networking and *in-silico* MS/MS fragmentation for natural products dereplication, Anal. Chem. 88 (2016) 3317–3323, https://doi.org/10.1021/acs.analchem.5b04804.
[61] J. Guo, H. Yu, S. Xing, T. Huan, Addressing big data challenges in mass spectrometry-based metabolomics, Chem. Commun. 58 (2022) 9979–9990, https://doi.org/10.1039/D2CC03598G.
[62] J.M. Gauglitz, K.A. West, W. Bittremieux, C.L. Williams, K.C. Weldon, M. Panitchpakdi, F. Di Ottavio, C.M. Aceves, E. Brown, N.C. Sikora, Enhancing untargeted metabolomics using metadata-based source annotation, Nat. Biotechnol. 40 (2022) 1–6, https://doi.org/10.1038/s41587-022-01368-1.
[63] D. Martins, S.d.S. Araújo, D. Rubiales, M.C. Vaz Patto, Legume crops and biotrophic pathogen interactions: a continuous cross-talk of a multilayered array of defense mechanisms, Plants 9 (2020) 1460, https://doi.org/10.3390/plants9111460.
[64] K.A. Aliferis, D. Faubert, S. Jabaji, A metabolic profiling strategy for the dissection of plant defense against fungal pathogens, PLoS One 9 (2014) e111930, https://doi.org/10.1371/journal.pone.0111930.
[65] F. Dakora, D. Phillips, Diverse functions of isoflavonoids in legumes transcend anti-microbial definitions of phytoalexins, Physiol. Mol. Plant Pathol. 49 (1996) 1–20, https://doi.org/10.1006/pmpp.1996.0035.
[66] A. Das, S. Choudhury, V. Gopinath, W. Majeed, S. Chakraborty, K.S. Bhairavi, S. Chowdhury, V.K. Dubey, M.S. Akhtar, Functions of flavonoids in plant, pathogen, and opportunistic fungal interactions, in: M.S. Akhtar (Ed.), Opportunistic Fungi, Nematode and Plant Interactions, Springer, Singapore, 2024, pp. 91–123.
[67] S. Steinkellner, R. Mammerler, Effect of flavonoids on the development of *Fusarium oxysporum* f. sp. *lycopersici*, J. Plant Interact. 2 (2007) 17–23, https://doi.org/10.1080/17429140701409352.
[68] L. Jiang, P. Wu, L. Yang, C. Liu, P. Guo, H. Wang, S. Wang, F. Xu, Q. Zhuang, X. Tong, Transcriptomics and metabolomics reveal the induction of flavonoid biosynthesis pathway in the interaction of *Stylosanthes-colletotrichum gloeosporioides*, Genomics 113 (2021) 2702–2716, https://doi.org/10.1016/j.ygeno.2021.06.004.
[69] R. Raman, S. Morris, N. Sharma, K. Hobson, K. Moore, Metabolite profiling of chickpea (*Cicer arietinum*) in response to necrotrophic fungus *Ascochyta rabiei*, Front. Plant Sci. 15 (2024) 1427688, https://doi.org/10.3389/fpls.2024.1427688.
[70] S.M. Mandal, D. Chakraborty, S. Dey, Phenolic acids act as signaling molecules in plant-microbe symbioses, Plant Signal. Behav. 5 (2010) 359–368, https://doi.org/10.4161/psb.5.4.10871.
[71] R. Lone, A. Bhat, N. Nazim, N.A. Malla, G.K. Rohella, H.I. Mohamed, Role of phenolics in plant-microbe interaction: a review, in: R. Lone, S. Khan, A. Mohammed Al-Sadi (Eds.), Plant Phenolics in Biotic Stress Management, Springer, Singapore, 2024, pp. 1–33.
[72] Y. Guo, J. Lv, Q. Zhao, Y. Dong, K. Dong, Cinnamic acid increased the incidence of Fusarium wilt by increasing the pathogenicity of *Fusarium oxysporum* and reducing the physiological and biochemical resistance of faba bean, which was alleviated by intercropping with wheat, Front. Plant Sci. 11 (2020) 608389, https://doi.org/10.3389/fpls.2020.608389.
[73] X. Yao, X. Sui, Y. Zhang, Amino acid metabolism and transporters in plant-pathogen interactions: mechanisms and implications, Plant Cell Environ. 48 (2025) 6086–6098, https://doi.org/10.1111/pce.15594.

[74] S. Fondevilla, N. Krezdorn, D. Rubiales, B. Rotter, P. Winter, Bulked segregant transcriptome analysis in pea identifies key expression markers for resistance to *Peyronellaea pinodes*, Sci. Rep. 12 (2022) 18159, https://doi.org/10.1038/s41598-022-22621-2.

[75] S. Liu, J. Jiang, Z. Ma, M. Xiao, L. Yang, B. Tian, Y. Yu, C. Bi, A. Fang, Y. Yang, The role of hydroxycinnamic acid amide pathway in plant immunity, Front. Plant Sci. 13 (2022) 922119, https://doi.org/10.3389/fpls.2022.922119.

[76] C.M. Rojas, M. Senthil-Kumar, V. Tzin, K.S. Mysore, Regulation of primary plant metabolism during plant-pathogen interactions and its contribution to plant defense, Front. Plant Sci. (2014) 5–17, https://doi.org/10.3389/fpls.2014.00017.

[77] M. Fagard, A. Launay, G. Clément, J. Courtial, A. Dellagi, M. Farjad, A. Krapp, M. C. Soulié, C. Masclaux-Daubresse, Nitrogen metabolism meets phytopathology, J. Exp. Bot. 65 (2014) 5643–5656, https://doi.org/10.1093/jxb/eru323.

[78] N.Q. Dong, H.X. Lin, Contribution of phenylpropanoid metabolism to plant development and plant–environment interactions, J. Integr. Plant Biol. 63 (2021) 180–209, https://doi.org/10.1111/jipb.13054.